Biochemical Pharmacology 79 (2010) 897–907

Contents lists available at ScienceDirect

Biochemical Pharmacology

journal homepage: www.elsevier.com/locate/biochempharm

Development of tolerance in D3 dopamine receptor signaling is accompanied by distinct changes in receptor conformation

Ligia Westrich [a], Sara Gil-Mast [a], Sandhya Kortagere [b], Eldo V. Kuzhikandathil [a,*]

[a] Department of Pharmacology & Physiology and Integrative Neuroscience Graduate Program, UMDNJ-New Jersey Medical School, Newark, NJ 07103, USA
[b] Department of Microbiology and Immunology, Drexel University College of Medicine, Philadelphia, PA 19129, USA

ARTICLE INFO

Article history:
Received 12 September 2009
Accepted 19 October 2009

Keywords:
Desensitization
Drd3
Modeling
Biotinylation
Signaling
GPCR

ABSTRACT

The D3 but not D2 dopamine receptors exhibit a tolerance property in which agonist-induced D3 receptor response progressively decreases upon repeated agonist stimulation. We have previously shown that the D3 receptor tolerance property is not mediated by receptor internalization, persistent agonist binding or a decrease in receptor binding affinity. In this paper, we test the hypothesis that alterations in D3 receptor conformation underlie the tolerance property. Structural models of wild type and mutant human D3 receptors were generated using the beta adrenergic receptor crystal structure as a template. These models suggested that the agonist-bound D3 receptor undergoes conformational changes that could underlie its tolerance property. To experimentally assess changes in receptor conformation, we measured the accessibility of native cysteine residues present in the extracellular and transmembrane regions of the human D3 receptor to two different thiol-modifying biotinylating reagents. The accessibilities of the native cysteine residues present in the D3 receptor were assessed under control conditions, in the presence of agonist and under conditions that induced receptor tolerance. By comparing the accessibility of D3 receptor cysteine residues to hydrophobic and hydrophilic thiol-modifying biotinylating reagents, we show that the alteration of D3 receptor conformation during tolerance involves the net movement of cysteine residues into a hydrophobic environment. Our results show that the conformation state of the D3 receptor during tolerance is distinct from the conformation under basal and agonist-bound conditions. The results suggest that the D3 receptor tolerance property is mediated by conformational changes that may uncouple the receptor from G-protein signaling.

1. Introduction

The dopamine receptors include D1 and D5 receptor subtypes (D1-like) and D2, D3, and D4 receptor subtypes (D2-like). D2 and D3 receptors modulate various signal transduction pathways via associated G-proteins [1]. Agonist stimulation of D2 and D3 receptors inhibits adenylyl cyclase and decreases cAMP production via Gαi/o subunit [2]. D2 and D3 receptors also couple to the mitogen-activated protein kinase (MAPK) pathway [3–5] and G-protein coupled inward rectifier potassium (GIRK) channels [6,7] via the βγ subunit of the heterotrimeric G-proteins.

By comparing the coupling of D2 and D3 dopamine receptors to endogenous GIRK channels and other effectors in AtT-20 cells, we previously demonstrated that the human D3, but not the D2 dopamine receptor exhibits tolerance and slow response termination properties [8,5] (Fig. 1). The D3 receptor tolerance property is defined as a progressive decrease in agonist-induced GIRK response upon repeated agonist stimulation. Typically, the magnitude of the second agonist-induced GIRK response is reduced by 60% compared to the first GIRK response [8,5] (Fig. 1). The slow response termination property of the D3 receptor describes the prolonged delay in termination of agonist-induced GIRK response after the removal of the agonist. The response termination rate of D3 receptor-induced GIRK response was 15-fold slower than the D2 receptor-induced GIRK response [8]. Together the tolerance and slow response termination properties distinguish D3 and D2 receptor signaling, which could be potentially important for normal physiological function. We have previously shown that the D3 receptor tolerance property is not mediated by receptor internalization, persistent agonist binding or a decrease in receptor binding affinity [8,5]. In this paper, using receptor modeling studies, we

* Corresponding author at: Department of Pharmacology & Physiology, UMDNJ-New Jersey Medical School, MSB, I-647, 185 South Orange Avenue, Newark, NJ 07103, USA. Tel.: +1 973 972 1157; fax: +1 973 972 4554.
E-mail address: kuzhikev@umdnj.edu (E.V. Kuzhikandathil).

0006-2952/$ – see front matter © 2009 Elsevier Inc. All rights reserved.
doi:10.1016/j.bcp.2009.10.016

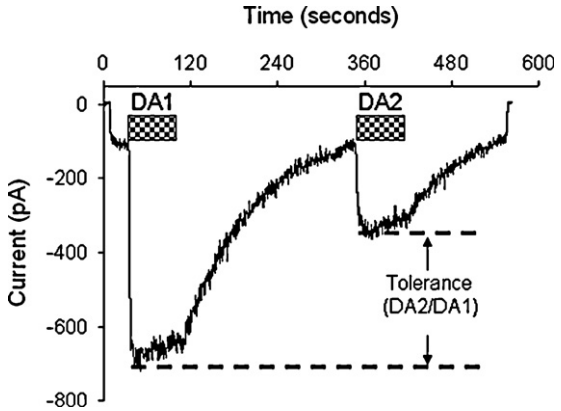

Fig. 1. Dopamine-induced tolerance. Representative current traces from whole cell voltage clamp recording of AtT-D3 cell. The cell was held at −65 mV and inward currents were elicited by two 1 min applications of 100 nM dopamine (DA, hatched rectangles). Tolerance is quantified as the ratio of second to first DA-induced GIRK current response.

determined that the conformational state of the wild type D3 receptor, which exhibits tolerance, is significantly different from a mutant D3 receptor that does not show tolerance. Similarly the conformational state of the wild type D3 receptor to tolerance- and non-tolerance-causing ligands are significantly different. These results led us to test the hypothesis that alterations in D3 receptor conformation underlie its tolerance property. To assess changes in receptor conformation we used a novel approach and measured the accessibilities of native cysteine residues present in the extracellular and transmembrane (TM) regions of the human D3 receptor to two different thiol-modifying biotinylating reagents (MTSEA- and TS-biotin-XX). The accessibilities of the native cysteine residues present in the D3 receptor were assessed under control conditions, in the presence of agonist and under conditions that induced receptor tolerance. The results show that the conformation state adopted by the D3 receptor, reflected by the relative alterations in cysteine accessibilities, is different under the three conditions. The results were confirmed by testing the cysteine accessibilities in a mutant D3 receptor that lacks tolerance and by using a D3 receptor agonist that does not elicit tolerance and slow response termination properties in wild type receptors. By comparing the accessibilities of D3 receptor cysteine residues to hydrophobic and hydrophilic thiol-modifying biotinylating reagents, we showed that the alteration of D3 receptor conformation during tolerance involves the net movement of cysteine residues into a hydrophobic environment. Together our results demonstrate that, unlike other dopamine receptor subtypes and many GPCRs, the termination of D3 receptor signaling is achieved by an alteration of receptor conformation.

2. Materials and methods

2.1. Cell culture and transfection

AtT-20 mouse pituitary cells were grown in Ham's F10 medium with 5% fetal bovine serum (FBS), 10% heat-inactivated horse serum, 2 mM glutamine and 50 μg/ml gentamicin (Invitrogen, Carlsbad, CA). AtT-20 cells stably expressing Flag™-tagged wild type D3 (AtT-Flag™ D3) or mutant C147K D3 (AtT-Flag™ D3C147K) dopamine receptor subtypes were maintained in the above F10 culture media supplemented with 500 μg/ml G418 (Invitrogen). For electrophysiological characterization, cells were plated onto glass coverslips coated with 40 μg/ml poly L-lysine (Sigma, St. Louis, MO) in a 12-well plate. All electrophysiological characterizations were carried out 36–48 h post-plating.

2.2. Electrophysiology, drugs, and solutions

Agonist-activated currents were measured by the whole cell patch clamp technique as described before [8]. Briefly, cells were held at −65 mV and inward K^+ currents induced by drug solutions were measured. The standard external solution (SES) used for K^+ current measurements was, in mM: 145 NaCl, 5 KCl, 2 $CaCl_2$, 1 $MgCl_2$, 10 Hepes [pH 7.4], and 10 glucose and the pipette solution contained in mM: 130 K-aspartate, 20 NaCl, 1 $MgCl_2$, 10 Hepes [pH 7.4], 10 glucose, 0.1 GTP, 5 Mg-ATP, and 1 EGTA. To enhance inwardly rectifying K^+ currents, controls and drug exposures were performed in solutions with elevated extracellular [K^+] (30 mM) by substitution for Na^+. Quinpirole and cis-8-hydroxy-3-(n-propyl)-1,2,3a,4,5,9b-hexahydro-1H-benz[e]indole hydrobromide (PBZI; Sigma) were dissolved in water and used at indicated concentrations. A 10 mM stock of dopamine (Sigma) was freshly dissolved in 100 mM ascorbic acid and used at a final concentration of 100 nM. Drug solutions were delivered to cells via a multi-barreled micropipette array. The current responses were normalized to the cell capacitance, to account for variation in cell size.

2.3. Data analyses

Currents were measured using an Axopatch 200B amplifier (Axon Instruments, Union City, CA, USA) and sampled through a Digidata 1322A interface (Axon Instruments) using the pClamp 8.0 software (Axon Instruments). Data files were imported into SigmaPlot (SPSS Inc., Chicago, IL) for analysis and display. SigmaPlot was also used to perform two-tailed Student's *t*-test. Analysis of variance (ANOVA) and the Holm's multiple pair-wise comparison tests were performed with Primer of Biostatistics software (Version 5.0, McGraw-Hill, New York, NY). Data were considered statistically different when probability was <0.05.

2.4. Biotin labeling of cysteine residues and immunoblotting of cell membrane proteins

AtT-Flag™ D3 or AtT-Flag™ D3C147K cells were harvested and treated with: (A) standard external solution (SES) for 1 min, or (B) pretreated with quinpirole or PBZI for 1 min, or (C) pretreated with quinpirole or PBZI for 1 min and then washed with SES for 5 min to remove agonists. Following the three treatment conditions, the cells were treated with four different concentrations of N-biotinylamino-ethylmethanethiosulfonate-XX (MTSEA-biotin) or biotin-XX ethylenediamine thiosulfate (TS-biotin) (Biotium, Hayward, CA) for 2 min. The XX-linker is incorporated to facilitate biotin–streptavidin interaction following the thiol modification. Stock solutions of MTSEA-biotin (50 mM) and TS-biotin (100 mM) were freshly prepared just before use in anhydrous DMSO (Sigma, catalog number 276855). Working stock solutions were prepared by further diluting the stock solutions in anhydrous DMSO. The concentrations of the working stock solutions were such that each treatment condition had the same final concentration of DMSO. The treatment scheme details are shown in Fig. 8. The concentrations of MTSEA/TS-biotin used were 0.02, 0.04, 0.06, and 0.1 mM. Excess MTSEA/TS-biotin was removed by washing the cells two times with SES. The final concentration of thiol biotinylating reagents were selected following extensive optimization experiments in which we varied the concentration of the biotinylating reagents from 0.01 mM to 1 mM and treated the cells for 1–10 min. Longer incubations and higher concentrations resulted in saturation under control conditions. The MTSEA/TS-biotin concentrations and time of treatment that were selected resulted in a consistent linear increase in biotinylated D3 proteins under control conditions.

To harvest AtT-Flag™ D3 and AtT-Flag™ D3C147K following treatment or immunoprecipitation we used Cell Lytic-M Cell Lysis Reagent (Sigma) with 10 μl/ml of protease inhibitor cocktail (Sigma) and 1 mM phenylmethanesulfonyl fluoride (PMSF) (Sigma). The biotinylated proteins were isolated following 1-h rotary incubation of 200 μg of total cell protein with 32 μl streptavidin-agarose beads (Pierce Biochemicals, Rockford, IL) at 4 °C. The supernatant was saved for further analysis of the cytosolic, non-biotinylated, proteins. The biotinylated membrane proteins attached to the streptavidin-agarose beads were eluted by incubation with 100 μl of gel loading buffer with 50 mM TCEP (Pierce Biochemicals) at 37 °C for 10 min. The eluted proteins were run on a 10% SDS-PAGE gel and transferred onto nitrocellulose membrane. The membrane was then stained using the MEMCode Reversible Protein Stain Kit (Pierce Biochemicals). Following removal of the stain, the membrane was probed with M2-Flag® primary antibody (1:2000; Sigma) and goat anti-mouse secondary antibody (1:20,000; Pierce Biochemicals). Both the primary and secondary antibodies were dissolved in 5% non-fat milk in Tris-buffered saline with 0.05% TWEEN®-20 (Sigma) and incubated with the membrane for 1 h at 25 °C. The Flag™-tagged D3 receptor was then detected by chemiluminescence using the West Dura™ kit (Pierce). The signal intensity was analyzed using gel densitometry system and software (Alpha Innotech Inc., San Leandro, CA). Each experiment was repeated three to five times and samples run in duplicate.

2.5. Molecular modeling and simulations

Structural models of the wild type and mutant (C147K and C147A) D3 dopamine receptor were modeled using the crystal structure of the beta adrenergic receptor (PDB code: 2RH1) [9] as a template to the homology modeling program Modeller (Ver. 9.4) [10]. Docking of PBZI and quinpirole was done using docking software Gold (Ver. 4.1) [11]. Twenty independent runs were performed for each ligand and the docked complexes were scored using goldscore [11], chemscore [12] and customized scoring scheme [13]. The customized scoring scheme was designed to identify correct binding modes of the ligand by scoring the known interactions such as the salt bridge with Asp110 and aromatic interactions with the aromatic residues from TM5, TM6 and TM7 positively and penalizing reversed binding modes. Finally the docked complexes were ranked based on a consensus scoring scheme described in detail in Kortagere et al. [13]. The wild type, C147K, C147A and the wild type receptor in complex with PBZI and quinpirole were further refined using energy minimization and molecular dynamics simulations. All simulations were performed using NAMD (Ver. 2) [14] with Charmm force field parameters [15]. A production run of 10 ns was used in all the simulations for further analysis. Residue based root mean square deviations were computed for the entire length of the trajectory for all simulations using VMD rmsd plugin [16]. Solvent accessible surface areas

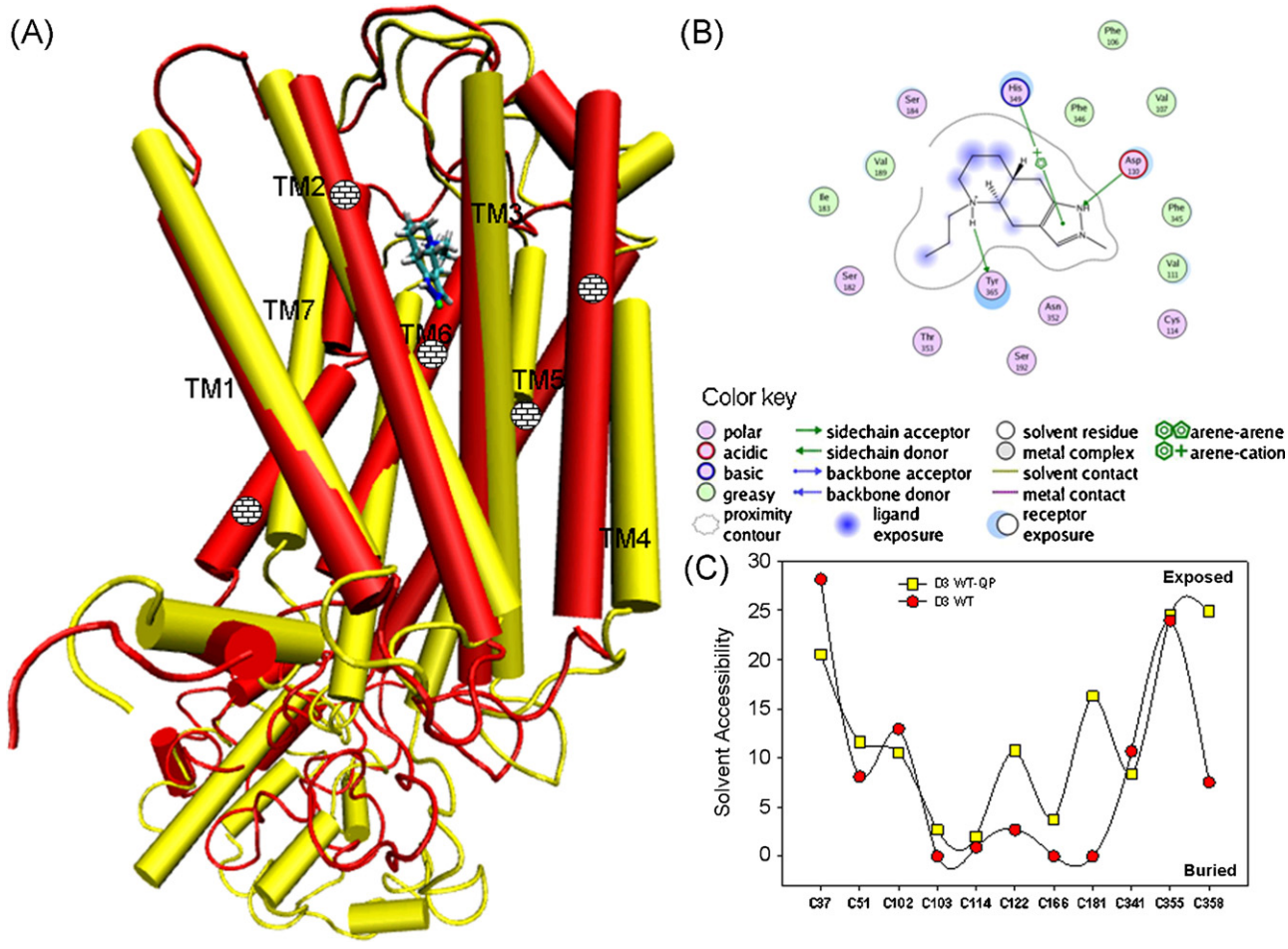

Fig. 2. Agonist-induced conformational changes in the model of wild type D3 receptor. (A) Structural super positioning of unbound (red) and quinpirole-bound form (yellow) of wild type D3 receptor are shown in cartoon representations with rods representing alpha helices and numbered TM1-7 and loops as coils. Circles with brick pattern represent approximate location of the proline residues in the TM helices. (B) Schematic representation of quinpirole binding to the D3 receptor model is shown. The figure was generated using the LigX application in MOE (Chemical Computing Group, Montreal, Canada). (C) Plot of solvent accessibility values of extracellular and transmembrane cysteine residues present in unbound and quinpirole (QP) bound wild type (WT) human D3 receptor. (For interpretation of the references to color in this figure legend, the reader is referred to the web version of the article.)

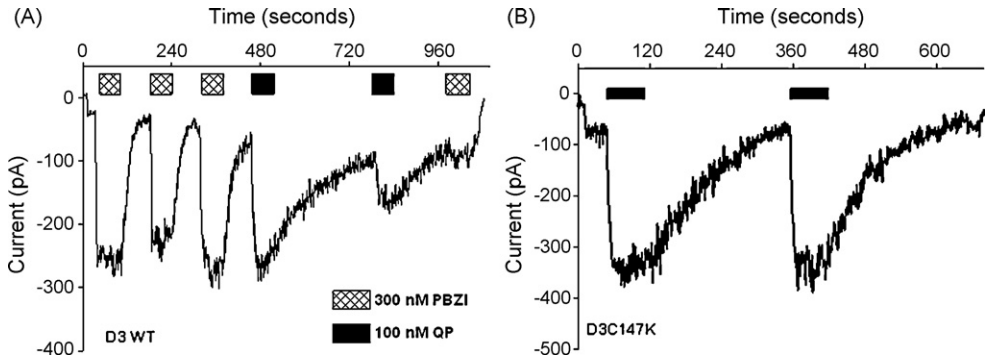

Fig. 3. An agonist that abolishes tolerance and a D3 receptor mutant that lacks tolerance. Representative voltage clamp recordings from AtT20 cells stably expressing either the wild type human D3 receptor (A) or the human D3 C147K mutant receptor (B). The cells were treated with either 300 nM PBZI (hatched rectangles) or 100 nM quinpirole (black rectangles). In cells expressing wild type D3 receptors, PBZI elicited three responses that did not show either tolerance or slow response termination properties; however, on the same cell, quinpirole elicited GIRK response with tolerance and slow response termination properties. Quinpirole does not elicit tolerance in cells expressing mutant D3 C147K receptors.

(SASA) were computed using Whatif program [17] and p*K*a values were computed using PROPKA program [18].

3. Results

3.1. D3 receptor modeling suggests agonist-induced changes in conformation could contribute to the tolerance property

The wild type D3 dopamine receptor was modeled based on the partial inverse agonist-bound conformation of the β2-adrenergic receptor and then refined using energy minimization and molecular dynamics simulations. The agonist quinpirole was next docked to the refined wild type D3 receptor model. Both bound and unbound wild type D3 receptor models were subjected to 10 ns long molecular dynamics simulations. Fig. 2B shows that quinpirole exhibits conserved salt bridge interactions with Asp110 and maintains aromatic interactions with residues from TM5 and TM6, similar to other dopamine receptor agonists. To facilitate these conserved interactions, the receptor undergoes major conformational changes at TM4, TM5, TM6 and EC3, and significant changes at the C-terminal end of TM3 and proline initiated kinked region of TM7 (Fig. 2A). In the quinpirole-bound form, the TM4 is found to open up the barrel with a movement of ~3.6 Å, while TM5 and TM6 twist by angle of 10–18° (Fig. 2A). The c-terminal ends of TM3 and TM7 rotate by angle of 5° and 8°, respectively. Changes in the measured SASA values of cysteines 122, 166 and 181 are consistent with these conformational changes (Fig. 2C). The changes in SASA values for the cysteine residues were also consistent with the changes in p*K*a values (data not shown). While the lack of homology in the loop region, in general, makes it difficult to accurately model the D3 loop regions, our modeling results suggest that EC3 of D3 receptor does exhibit significant agonist-dependent changes relative to EC1 and EC2. The results from the modeling studies not only show the expected agonist-induced alterations in the D3 receptor conformation but also identify potential regions such as TM3, TM4 and EC3, which are likely to be involved in the conformational change.

The tolerance property of the D3 receptor is abolished in the D3C147K mutant receptor and is also dependent on the type of agonist. We have determined that certain D3 receptor agonists such as cis-8-OH-PBZI (PBZI) do not elicit the tolerance and slow response termination properties (Fig. 3A). Similarly, we have previously shown that a single point mutation, C147K, in the D3 receptor second cytoplasmic loop selectively abolishes the tolerance property (Fig. 3B) [5]. In contrast, a C147A mutation in the D3 receptor retains tolerance and slow response termination properties [5]. We used the modeling approaches described in Fig. 2, to compare the conformational state of the wild type or a mutant D3 receptor, which exhibit tolerance, and a tolerance-lacking mutant D3 receptor. Specifically, we determined solvent accessibilities of the cysteine residues in the wild type D3 receptor, the D3 C147K mutant that lacks tolerance and the control D3C147A mutant that retains wild type tolerance. In addition, we also determined if the conformation changes elicited by non-tolerance-causing agonist (PBZI) were different from agonists such as quinpirole that elicit tolerance. The results in Fig. 4A show that several of the cysteine residues in the D3 C147K mutant exhibit altered solvent accessibility compared to D3C147A and wild type D3 receptor. The SASA values for the cysteine residues in the unbound tolerance-lacking D3C147K mutant receptor are distinctly different from the wild type and D3C147A mutant receptors which exhibit tolerance. Similarly the solvent accessibilities of cysteine residues in quinpirole-bound D3 receptor are different from the PBZI-bound D3 receptor (Fig. 4B). Compared to the

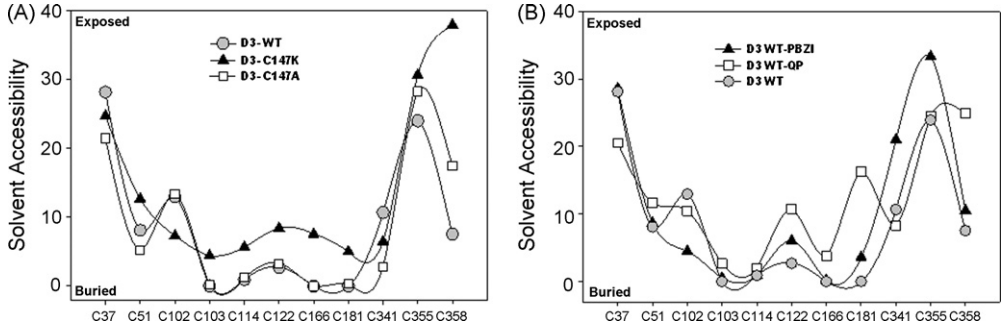

Fig. 4. Solvent accessible surface areas (SASA) values of extracellular and transmembrane cysteine residues. (A) SASA values of wild type D3 receptor (D3 WT), mutant D3 C147K (D3-C147K) and mutant D3 C147A (D3-C147A) receptor models. (B) SASA values for unbound wild type D3 receptor (D3 WT), or wild type D3 receptor bound by quinpirole (D3 WT-QP) or PBZI (D3 WT-PBZI). High and low SASA values correspond to exposed or buried residues, respectively.

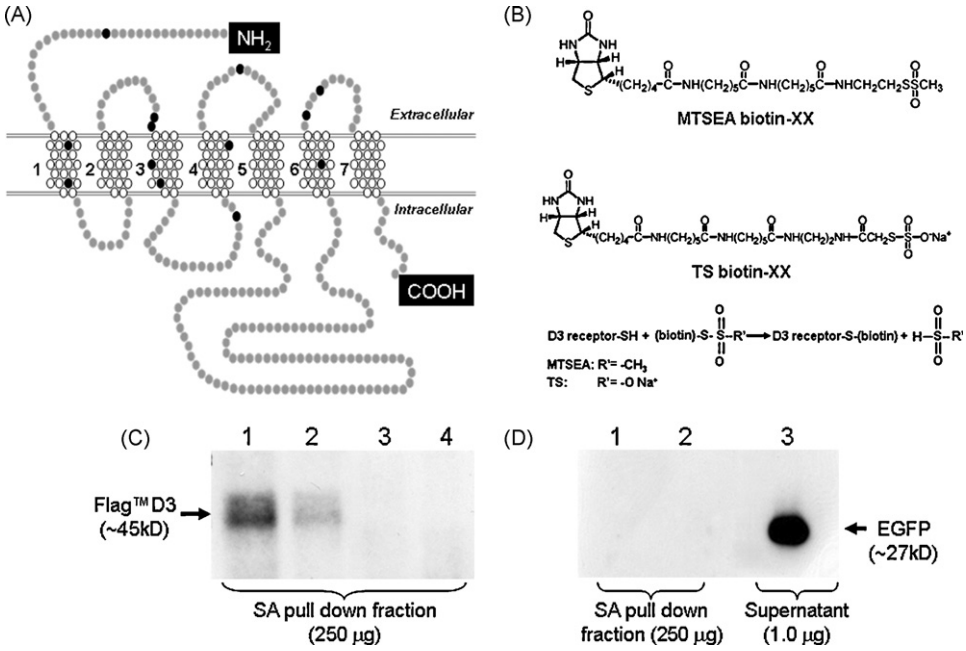

Fig. 5. Diagram of the D3 receptor with putative cysteine residues that can be biotinylated by thiol-reactive reagents. (A) The black ovals represent putative locations of the 12 cysteine residues found in the extracellular (gray ovals) or transmembrane regions (white ovals). A 13th cysteine residue (C147) of D3 receptor is shown in the second intracellular region of the membrane. (B) Chemical structures of thiol-modifying reagents MTSEA-biotin-XX and TS-biotin-XX, and the chemical reaction that leads to biotinylation of the D3 receptor. (C) Representative Western blot showing the streptavidin agarose (SA) pull-down fraction from AtT-Flag^{TM} D3 cells treated with 1 mM MTSEA (lane 1), 0.3 mM MTSEA (lane 2), 0.6% DMSO (lane 3) and AtT-20 cells treated with 1 mM MTSEA (lane 4) as control. The D3 receptor was detected using anti-Flag^{TM} monoclonal antibody. (D) Representative Western blot showing the streptavidin (SA) pull-down fraction from AtT-Flag^{TM} D3 cells treated with 1 mM MTSEA (lane 1), 0.3 mM MTSEA (lane 2) and the supernatant fraction from AtT-Flag^{TM} D3 cells treated with 1 mM MTSEA (lane 3). The EGFP stably expressed in the cells was detected using anti-EGFP monoclonal antibody.

quinpirole-docked wild type receptor, the conformational variations in the PBZI-docked wild type receptor complex resembled the unbound wild type D3 receptor. Together the results from the modeling studies suggest that D3 receptor exhibits distinct and tolerance-specific conformational states.

3.2. Thiol-reactive biotinylation reagents specifically label cell surface proteins

To determine if the tolerance-specific D3 receptor conformation could be experimentally detected, we adapted a technique that has been previously used to monitor conformational states of ion channels and to identify residues lining the binding pocket in receptors [19,20]. The D3 receptor contains 12 native cysteine residues in the extracellular and transmembrane regions (Fig. 5A). We decided to monitor the changes in D3 receptor conformation during control, agonist-treated and tolerance conditions by measuring the accessibility of the native cysteine residues to two different thiol-modifying biotinylating reagents. We used two thiol-reactive biotinylating reagents, the non-charged MTSEA-biotin-XX and the negatively charged TS-biotin-XX, to introduce a biotin tag into the protein during the cysteine modification reaction (Fig. 5B). The biotinylated proteins can be efficiently precipitated using streptavidin-linked agarose beads and run on a Western gel and detected with an antibody for the specific protein. The amount of protein detected on the Western gel is directly proportional to the biotin incorporated into the protein by the MTSEA-biotin reagent during the cysteine modification. The XX spacer between the biotin and thiol-reactive moieties facilitates the interaction between biotin and streptavidin. Due to their size, these reagents are not expected to penetrate the cellular membrane and biotinylate intracellular proteins. In addition, TS-biotin is less likely to enter the membrane and biotinylate cysteine residues embedded in the membrane due to its negative charge. Before using these reagents, we decided to test the above mentioned features of these reagents and optimize the conditions for using this method to detect D3 receptor conformation changes.

To demonstrate the specificity of biotin labeling of the D3 receptor using the MTSEA-biotin reagent, non-transfected parental AtT-20 cells and AtT-Flag^{TM} D3 cells were treated with vehicle (DMSO) or two relatively high concentrations of MTSEA-biotin for 10 min. Following lysis, labeled proteins were pulled down using streptavidin agarose, washed, eluted and separated by SDS-PAGE. The Flag^{TM} tagged D3 receptor was detected using an anti-Flag^{TM} monoclonal antibody. Fig. 5C shows that MTSEA-biotin specifically labels the Flag^{TM} tagged D3 receptor in a dose-dependent manner (lanes 1 and 2). Vehicle treated AtT-Flag^{TM} D3 cells (lane 3) and parental non-transfected AtT-20 cells treated with 1 mM MTSEA-biotin (lane 4) did not reveal any biotin-labeled proteins on the gel. These results demonstrate that the D3 receptor can be biotinylated using the MTSEA-biotin in a dose-dependent manner.

As mentioned above, both MTSEA- and TS-biotin are not expected to label intracellular proteins; we tested this directly using AtT-Flag^{TM} D3 cells treated with 1 mM or 0.3 mM MTSEA-biotin for 10 min. MTSEA-biotin has a neutral charge and is more likely to be cell permeable. The AtT-Flag^{TM} D3 cells are engineered to co-express the cytosolic enhanced green fluorescent protein (EGFP); therefore, we measured the ability of MTSEA-biotin to label the cysteine residues present in this cytosolic protein. In Fig. 5D we demonstrate that, under our experimental conditions, MTSEA-biotin does not label the cysteine residues of the cytosolic EGFP. Protein lysates from cells treated with 1 or 0.3 mm MTSEA-biotin and pulled down with streptavidin agarose did not reveal any biotin-labeled EGFP protein (lanes 1 and 2). In contrast, lane 3 shows that the supernatant from the pulled down contained significant amount of EGFP. These results confirm that the MTSEA-biotin reagent does not label cytosolic proteins under our experimental conditions. Furthermore, in subsequent experiments, we used a maximum concentration of 0.1 mM MTSEA-biotin which is 10-fold less than the amount used in the

(A)

CONTROL

MTSEA (mM)	EC-1 (15)	TM-1 (37)	TM-1 (51)	EC-2 (102)	EC-2 (103)	TM-3 (114)	TM-3 (122)	TM-4 (166)	EC-3 (181)	TM-6 (341)	EC-4 (355)	EC-4 (358)	Total	Relative
0.02	0	1	0	0	0	0	0	0	0	0	1	0	2.0	1.0
0.04	1	1	0	1	0	0	0	0	0	0	1	0	4.0	2.0
0.06	1	1	1	1	0	0	0	0	0	1	1	1	7.0	3.5
0.10	1	1	1	1	0	0	1	0	0	1	1	1	8.0	4.0

QUINPIROLE

MTSEA (mM)	EC-1 (15)	TM-1 (37)	TM-1 (51)	EC-2 (102)	EC-2 (103)	TM-3 (114)	TM-3 (122)	TM-4 (166)	EC-3 (181)	TM-6 (341)	EC-4 (355)	EC-4 (358)	Total	Relative
0.02	1	1	1	0	0	0	0	0	1	0	1	1	6.0	1.0
0.04	1	1	1	1	0	0	1	0	1	1	1	1	9.0	1.5
0.06	1	1	1	1	0	0	1	0	1	1	1	1	9.0	1.5
0.10	1	1	1	1	0	0	1	1	1	1	1	1	10.0	1.7

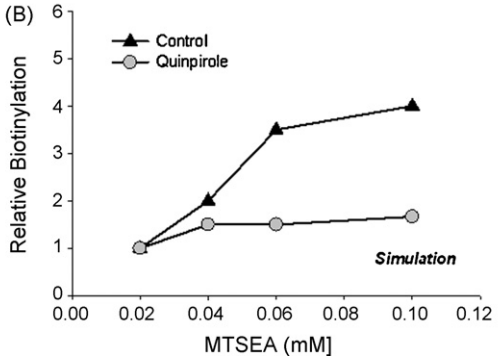

Fig. 6. Hypothetical model representing MTSEA-biotinylation of D3 receptor under control and quinpirole-treated conditions. (A) Putative D3 receptor cysteine residues that are accessible and biotinylated at the specified MTSEA concentrations are designated with a 1, while those that are not accessible are designated with a 0. This is based on the putative arrangement of 12 cysteine residues in the extracellular and transmembrane regions of the D3 receptor and from the SASA values. (B) Simulation of relative biotinylation levels under control and quinpirole-treated conditions at various MTSEA concentrations. This is based on the total number of cysteines that are potentially biotinylated under control and quinpirole-treated conditions and is derived from the table in (A).

experiments shown in Fig. 5. In addition, the duration of biotin labeling was decreased from 10 min to 2 min.

3.3. Using thiol-reactive biotinylation reagents to monitor relative changes in D3 receptor conformation

The wild type D3 receptors contain 16 cysteine residues of which 6 are in the extracellular regions, 6 are in the transmembrane regions and 4 are in the cytoplasmic regions. Any change in conformation of the receptor can potentially alter the accessibility of the 12 cysteine residues in the extracellular and transmembrane regions to the sulfhydryl reagent MTSEA. To determine the theoretical outcome of differential biotinylation of the cysteine residues, we performed a simple simulation. The representative example in Fig. 6 shows the predicted result from a theoretical cysteine modification experiment wherein the accessibilities of cysteine residues are altered in the presence of the agonist, quinpirole. The simulation in Fig. 6 assumes that there are 12 cysteine residues in D3 receptor that are potentially accessible to thiol-modifying reagents. The simulation also assumes that a residue that is biotinylated at a particular concentration will also be biotinylated with a higher concentration of the reagent. Unmodified cysteines are assigned a value of zero and modified cysteine residues a value of one (Fig. 6A). In the example shown in Fig. 6, four different concentrations of the MTSEA-biotin reagent are used to treat cells in the absence or presence of the D3 receptor agonist quinpirole. The outcome of the simulation is shown in Fig. 6B where the relative number of cysteines biotinylated in the D3 receptor protein is plotted versus increasing concentration of the MTSEA reagent. When the ligand quinpirole is added to the receptor, this simulation assumes that there is a change in accessibility of the cysteine residues to the MTSEA reagents. The changes in accessibility used in the simulation are loosely based on the solvent accessibility plots of unbound and quinpirole-bound wild type D3 receptor shown in Fig. 2C. The simulated plots expected in the presence and absence of quinpirole is shown in Fig. 6B and shows a significant difference in the slope.

Next, to experimentally verify the model, we treated AtT-20 cells stably expressing the D3-Flag receptor with four different concentrations (0.02, 0.04, 0.06 and 0.1 mM) of MTSEA-biotin reagent in the absence or presence of 100 nM quinpirole for 2 min. After extensive washing to remove excess MTSEA reagent, cells were lysed and biotinylated proteins pulled down with streptavidin-agarose beads, run on Western gel and probed with a Flag antibody (Fig. 7A). The results in Fig. 7B show that in the presence of quinpirole there is the predicted occlusion and changes in accessibilities of the cysteine residues, resulting in a saturated level of biotinylation. The relative difference in the biotinylation rate between unbound and bound D3 receptor is indicated by the significantly different slopes of the biotinylation curve (Fig. 7C). For quantification the ratio of biotinylated D3 receptors in cells treated with 0.1 mM and 0.02 mM MTSEA-biotin was determined. Fig. 7D shows that this ratio is significantly different between control and quinpirole treated cells. Together the results in Fig. 7 showed that biotinylation rate in quinpirole-bound D3 receptor samples is significantly less than in unbound D3 receptor samples. The changes in biotinylation induced by the presence of quinpirole are specific for the D3 receptor as total protein stain of the same nitrocellulose blot using the Memcode™ reversible protein stain revealed that other biotinylated membrane proteins that were co precipitated by streptavidin agarose showed a MTSEA-biotin concentration-dependent linear increase in the absence and presence of quinpirole (Fig. 7A). Comparing the biotinylation rate results from Figs. 6B and 7C, the theoretical simulation results match the experimental results. However, the absolute biotinylation levels observed in the simulation is different from the experimental results. This is likely due to inherent differences between theoretical biotinylation of a single receptor in the

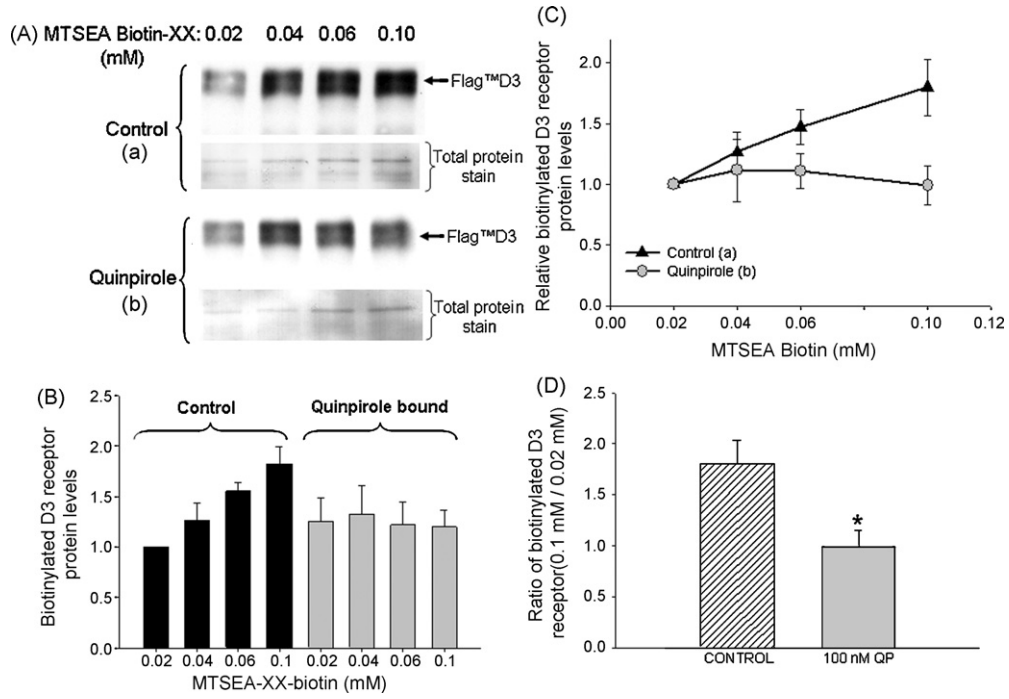

Fig. 7. Accessibility of D3 receptor cysteine residues to thiol-modifying reagents is reduced in the presence of quinpirole. (A) Representative Western blots showing Flag™D3 receptor that has been treated with increasing concentrations of MTSEA-biotin under control (a) and quinpirole-bound (b) conditions. A non-specifically biotinylated protein is detected on the same blot using a total protein stain (MEMCode reversible stain). (B) Cumulative biotinylated Flag™-tagged D3 receptor protein levels measured relative to the biotinylated Flag™-tagged D3 receptor levels in the 0.02 mM MTSEA-biotin treated control samples. Biotinylated Flag™-tagged D3 receptor protein levels in control (black) and quinpirole-bound (gray) conditions are shown. (C) Relative biotinylation rate of Flag™-tagged D3 receptor protein levels under control (black triangles) and quinpirole-bound (gray squares) conditions at increasing MTSEA-biotin concentrations. The levels are relative to the lowest concentration (0.02 mM), which is set to 1. (D) The ratios of biotinylated Flag™-tagged D3 receptor at the highest (0.1 mM) to the lowest (0.02 mM) MTSEA concentration for quinpirole-bound (in the presence of quinpirole) and control conditions are statistically different ($^*P < 0.05$, Student's *t*-test).

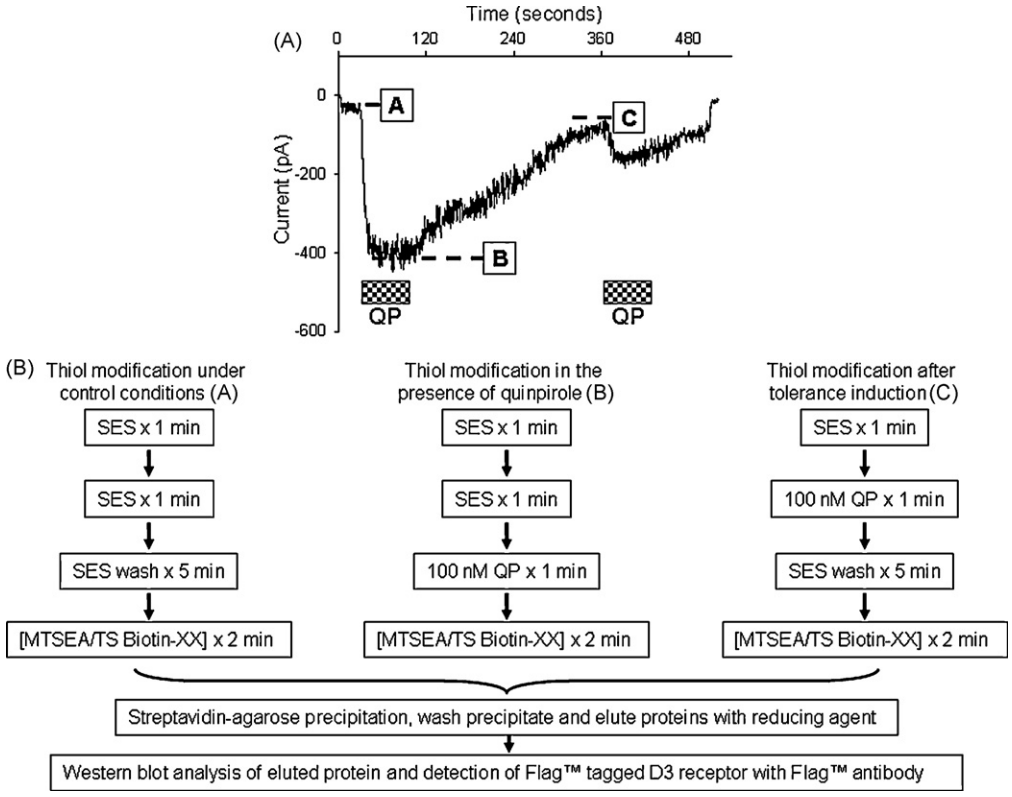

Fig. 8. The treatment conditions used for the biotinylation experiment match those used in the electrophysiology studies. (A) Representative current trace from whole cell voltage clamp recording of AtT-D3. The cell was held at −65 mV and inward currents elicited by 1-min applications of 100 nM quinpirole (checkered rectangles). The boxed letters A, B, and C represent the points at which we added the MTSEA/TS-biotin reagents as outlined in (B).

simulation versus the actual biotinylation of a population of receptors under experimental conditions. The differences could also arise due to steric hindrances encountered by the bulky biotinylating reagent during thiol modification due to the presence of quinpirole in the receptor binding pocket. Together these results suggest that the MTSEA-biotin modification approach can be used to test the accessibilities of native cysteine residues present in the D3 receptor. In turn, the change in cysteine accessibilities under different treatment conditions reflects the alterations in D3 receptor conformation; therefore this approach can be used to monitor the conformation state of the D3 receptor.

3.4. D3 receptor tolerance property is associated with a novel receptor conformation state

We hypothesized that if there were changes in the conformation of the D3 receptor following agonist-induced tolerance, there would be changes in the accessibility of various cysteine residues present in the receptor. Some cysteine residues might get embedded in the membrane, becoming less accessible to the thiol-modifying biotinylation reagents; others might get exposed to the extracellular environment becoming more available for thiol modification; yet others might show no changes in accessibility. The overall biotinylation levels of Flag™D3 receptors under control, agonist-treated, and tolerance conditions was assessed and compared at various concentrations of the thiol-reactive reagents. The scheme used for executing these experiments is described in Fig. 8. In the case of D3 receptors that are induced to undergo tolerance, the agonist was thoroughly washed out for 5 min. This time period was chosen based on the functional experiments which showed that the agonist-induced response had terminated and returned to baseline in approximately 5 min [5,8]. If the receptor returned to its original (basal) conformation following the 5 min wash out, the accessibilities of the cysteine residues should not be altered and we would expect to detect the same biotinylation rate as in control samples. In contrast, if the D3 receptor adopted a different conformation after the 5 min wash out, embedding or exposing some cysteine residues, we would expect to see alterations in cysteine accessibilities and consequently a different biotinylation rate compared to control samples.

The Western blot results in Fig. 9A show that following agonist treatment and the 5 min wash out, the tolerant D3 receptor exhibits significantly more biotinylation by MTSEA-biotin. This is quantitated in the cumulative results shown in Fig. 9B. The results suggest that under quinpirole-induced tolerance, more cysteine residues in the D3 receptor are biotinylated compared to control conditions; however, this occurs only at higher MTSEA-biotin concentrations. The relative biotinylation rate pattern (Fig. 9C) suggests that following quinpirole treatment and washout, after tolerance is induced, the D3 receptor exhibits a novel conformation that is different from its basal conformation. In this novel conformation more native cysteine residues are apparently biotinylated by the MTSEA-biotin reagent (Fig. 9D).

3.5. The novel conformation state is specifically related to D3 receptor tolerance

While the results in Fig. 9 suggest altered cysteine accessibilities in a D3 receptor that is in a tolerant state, it does not indicate if the underlying receptor conformation is specific to D3

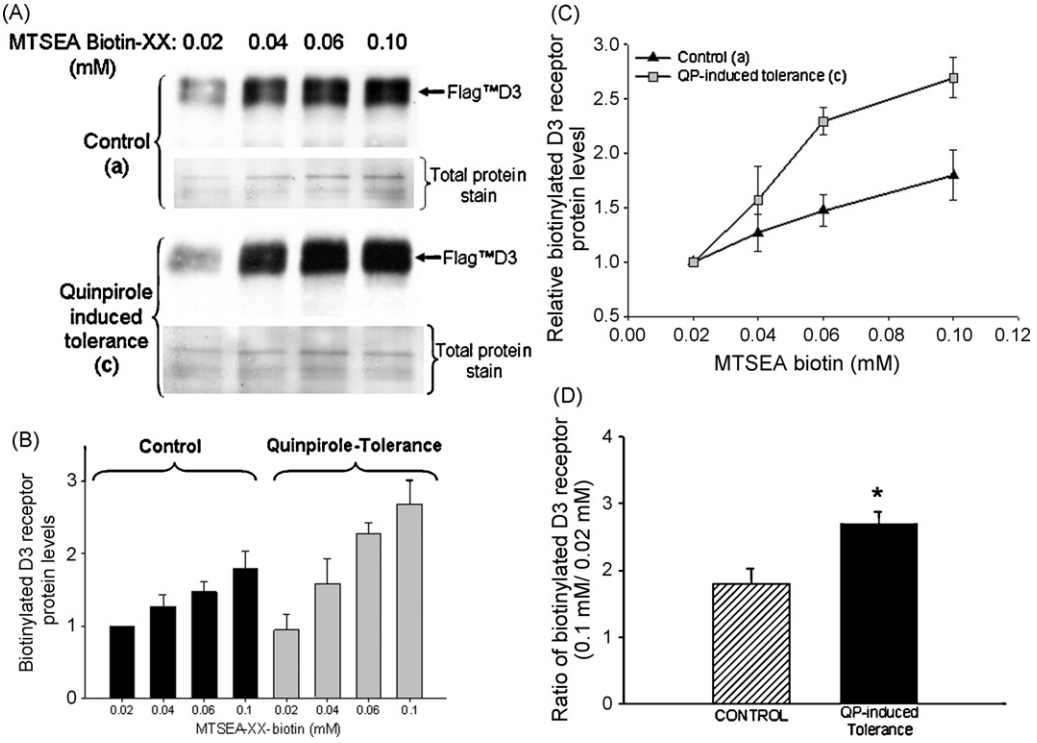

Fig. 9. Accessibility of D3 receptor cysteine residues to thiol-modifying reagents is altered upon quinpirole-induced tolerance. (A) Representative Western blots showing Flag™D3 receptor that has been treated with increasing concentrations of MTSEA-biotin under control and quinpirole-induced tolerance conditions. A non-specifically biotinylated protein is detected on the same blot using a total protein stain (MEMCode reversible stain). (B) Cumulative biotinylated Flag™-tagged D3 receptor protein levels measured relative to the biotinylated Flag™-tagged D3 receptor levels in the 0.02 mM MTSEA-biotin treated control samples. Biotinylated Flag™-tagged D3 receptor protein levels in control (black) and quinpirole-induced tolerance (gray) conditions are shown. (C) Relative biotinylation rate of Flag™D3 receptor protein levels under control (black triangles) and quinpirole-induced tolerance (gray squares) conditions at increasing MTSEA-biotin concentrations. The levels are relative to the lowest concentration (0.02 mM), which is set to 1. (D) The ratios of biotinylated Flag™-tagged D3 receptor at the highest (0.1 mM) to the lowest (0.02 mM) MTSEA-biotin concentration for quinpirole-induced tolerance and control conditions are statistically different (*$P < 0.05$, Student's t-test). Note that the control samples shown in this figure are identical to that in Fig. 7.

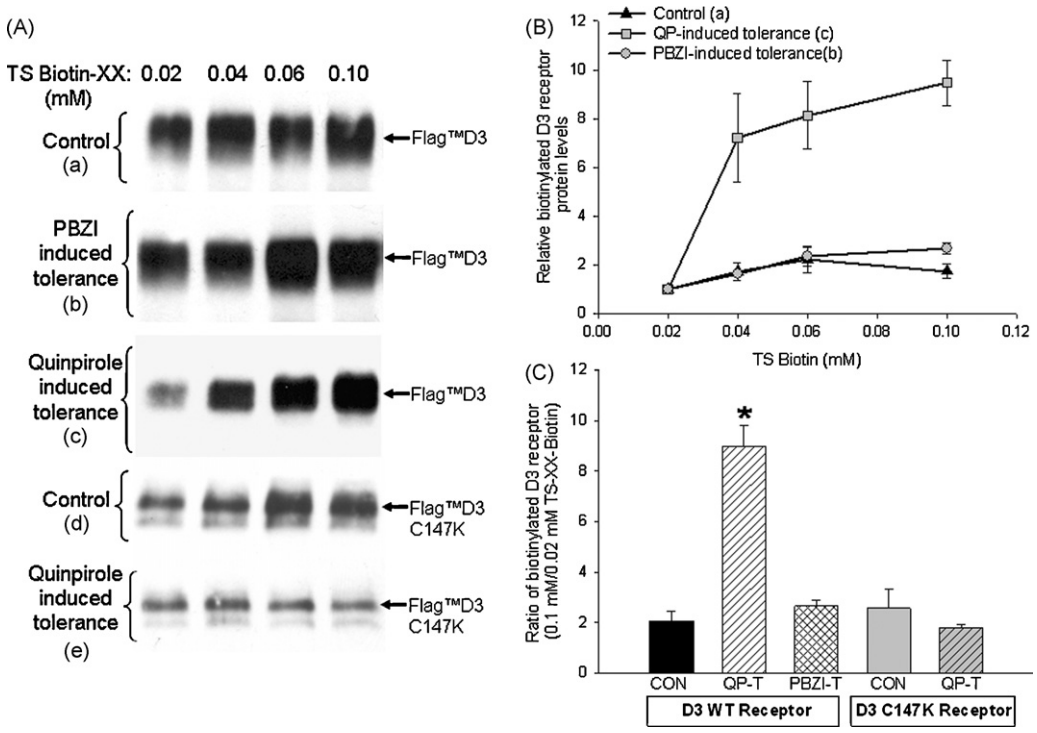

Fig. 10. TS-biotin-XX mediated biotinylation of D3 receptor distinguishes D3 receptors that undergo tolerance versus receptors that do not exhibit tolerance. (A) Representative Western blots showing Flag™D3 wild type or Flag™D3 C147K receptor that has been treated with increasing concentrations of TS-biotin under control, quinpirole-, and PBZI-induced tolerance conditions. (B) Relative biotinylation rate of Flag™D3 receptor protein levels under control (black triangles), quinpirole-induced tolerance (gray squares), and PBZI-induced tolerance (gray circles) conditions at increasing MTSEA-biotin concentrations. The levels are relative to the lowest concentration (0.02 mM), which is set to 1. (C) The mean ratios of biotinylated D3 receptor at the highest (0.1 mM) to the lowest (0.02 mM) MTSEA-biotin concentration for quinpirole-induced tolerance conditions are statistically different than control, mutant D3 C147K and PBZI-induced tolerance conditions (*$P < 0.05$, ANOVA, post hoc Holm's test).

receptor that is in a tolerant state. To determine this, we used two different approaches. We have observed that certain D3 receptor agonists such as cis-8-OH-PBZI (PBZI) do not elicit the tolerance and slow response termination properties (Fig. 3A). Similarly, we have previously shown that a single point mutation, C147K, in D3 receptor second cytoplasmic loop selectively abolishes the tolerance property (Fig. 3B) [5]. We hypothesized that if the conformation adopted by the D3 receptor during tolerance results in the distinct cysteine accessibility pattern shown in Fig. 9, then agonists such as PBZI that do not elicit tolerance should exhibit a cysteine modification pattern that is unlike the pattern in Fig. 9 but similar to control conditions. Similarly the C147K mutant D3 receptor that lacks tolerance, should exhibit a cysteine accessibility pattern that is different from the wild type D3 receptor.

To experimentally test the hypothesis, we used the negatively charged cysteine modification reagent, TS-biotin, as it was less likely to interact with the cysteine residues in a hydrophobic environment compared to MTSEA-biotin. In Fig. 10 we show that the biotinylation pattern of D3 receptors treated with PBZI, under conditions that mimic those used for inducing tolerance, is significantly different from quinpirole-induced tolerance and more comparable to control conditions when the receptor had not been treated with agonists (Fig. 10A and B). Similarly, the cysteine modification and biotinylation pattern of D3C147K

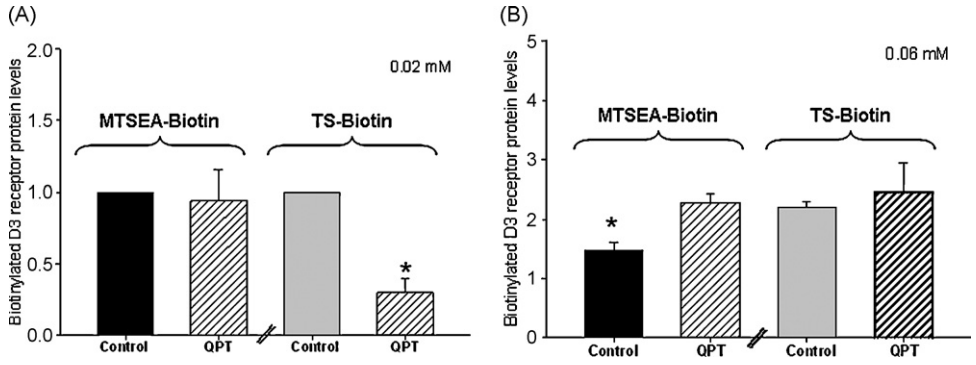

Fig. 11. During quinpirole-induced tolerance the accessibility of D3 receptor cysteine residues is different for MTSEA- and TS-biotin reagents. (A) The mean ratios of biotinylated Flag™-tagged D3 receptor at the lowest (0.02 mM) MTSEA-biotin and TS-biotin concentrations for control and quinpirole-induced tolerance (QPT) conditions. (B) The mean ratios of biotinylated Flag™-tagged D3 receptor at a higher (0.06 mM) MTSEA-biotin and TS-biotin concentrations for control and quinpirole-induced tolerance (QPT) conditions. At 0.06 mM MTSEA-biotin concentration, but not at the 0.02 mM MTSEA-biotin concentration, the level of biotinylated Flag™-tagged D3 receptor is significantly increased for the quinpirole-induced tolerance condition compared to the control. Conversely, at 0.02 mM TS-biotin concentration, but not at the 0.06 mM TS-biotin concentration, the level of biotinylated Flag™-tagged D3 receptor is significantly decreased for the quinpirole-induced tolerance condition compared to the control condition (*$P < 0.05$, Student's t-test).

mutant receptor that was treated with quinpirole and washed under conditions that elicit tolerance in the wild type D3 receptor again revealed that the biotinylation was similar to control conditions and significantly different from that observed with wild type D3 receptors (Fig. 10A and C).

Together these cysteine accessibility results strongly suggest that the wild type D3 receptor, that has undergone tolerance, adopts a unique tolerance-specific conformation.

3.6. Tolerance-associated changes in D3 receptor conformation involves movement of cysteine residues located at the interface of hydrophobic and hydrophilic regions

Based on the putative topology of the D3 receptor (Fig. 5A), there are several cysteine residues that are found at the interface between the membrane and extracellular space. These putative cysteine residues can become accessible or embedded depending on the conformation of the D3 receptor. To ascertain the net movement of the cysteine residues following the induction of tolerance, we compared the ability of the neutral MTSEA-biotin and negatively charged TS-biotin to biotinylate D3 receptors under control and quinpirole-induced tolerance conditions. The results in Fig. 11 show that at the lowest concentration of MTSEA-biotin, the level of biotinylated D3 receptor was equal between control and quinpirole-induced tolerance conditions. In contrast, at the lowest concentration of TS-biotin the level of biotinylated D3 receptor was significantly decreased in quinpirole-induced tolerance conditions compared to control conditions. The differences observed at higher concentrations of MTSEA- and TS-biotin were less significant. Together these results suggest that during tolerance there is a net movement of cysteine residues from a relatively hydrophilic environment to a hydrophobic environment. At the lowest concentration, the MTSEA-biotin, but not the TS-biotin, is able to biotinylate the cysteine residues in this hydrophobic environment.

4. Discussion

The D3 dopamine receptor has been implicated in various neuropsychiatric and neurological disorders. All antipsychotics and most drugs used to treat Parkinson's disease have high affinity for D3 receptors. Unlike D1 and D2 dopamine receptors, the signaling mechanisms and properties of D3 receptors are not well understood [2]. We have previously reported that the D3 receptor exhibits tolerance and slow response termination properties and identified some of the key residues in the D3 receptor that is involved in the tolerance property [5,8]. Unlike receptor desensitization, which occurs in the continuous presence of an agonist, tolerance is defined as the termination or attenuation of receptor signaling upon repeated agonist stimulation. The D3 receptor does not exhibit significant desensitization but instead exhibits robust tolerance. The mechanisms by which D1 and D2 dopamine receptor signaling undergoes desensitization have been well described [21]. However, the molecular mechanisms underlying D3 receptor tolerance property remain to be determined. We have shown that tolerance property is not mediated by classical desensitization mechanisms such as receptor internalization [8], persistent agonist binding or a reduction in binding affinity [5,8]. In this paper, we tested the hypothesis that during tolerance, the D3 receptor undergoes a conformational change that may uncouple the receptor from G-protein signaling. Specifically, we tested a key element of the hypothesis that there is a change in conformation during tolerance. We used both modeling and a novel experimental approach to demonstrate that the D3 receptor adopts a distinct conformation when it undergoes tolerance.

For the modeling experiments we used the data obtained from the crystal structure of the β2-adernergic receptor [9] to develop a D3 receptor model. The model exhibited conformation changes upon agonist binding and demonstrated alterations in the solvent accessible surface area values of key cysteine residues. More interestingly, when we compared the structural models and SASA values of unbound wild type D3 receptor, D3 C147A receptor and the D3 C147K receptor, the tolerance-lacking D3C147K mutant receptor was significantly different from either the wild type or the mutant C147A D3 receptor that exhibits tolerance (Fig. 4A). Similarly, when we compared the quinpirole- or PBZI-bound wild type D3 receptor, the SASA values of the tolerance and slow response termination-inducing quinpirole was very different from that of PBZI, an agonist that does not induce either of these properties (Fig. 4B).

The modeling approach while providing an insight into the potential conformation of the unbound and bound receptor, does not allow us to predict the specific conformation that the receptor adopts during tolerance. This is because the tolerance state of the D3 receptor develops *after* the bound agonist has been washed out over a 5 min-period. The tolerance of the D3 receptor develops after the activation of a signaling cascade that likely involves alterations in the phosphorylation state of the receptor. To identify the distinct tolerance-associated conformational state, we adapted an approach that has been extensively used to probe conformational states of ion channels and map the residues in the binding pocket of receptors [19,20]. In the traditional substituted cysteine accessibility method (SCAM), cysteine residues are introduced at various positions in the protein using site-directed mutagenesis and their ability to react with sulfhydryl methanethiosulfonate reagents determined using functional or ligand binding assays [19,20]. Modification of the cysteine residues that impact ligand binding, conductance or gating properties provides information about the amino acid residue and/or protein domains involved in the function of the protein. However, SCAM has drawbacks, particularly if the substituted cysteines result in alterations of receptor conformation and potentially the signaling function. In this paper we report a novel adaptation of this approach wherein we use sulfhydryl reagents that transfer a biotin molecule to each of the accessible native cysteine residues present in the D3 receptor. The ability of sulfhydryl reagents to label the receptor with biotin is dependent on the accessibility of the cysteine residue, the concentration of the sulfhydryl reagent and the time of incubation. After initial optimization we fixed the time of treatment and determined the accessibility of the cysteine residues under control, agonist bound and tolerance conditions to four different concentration of the sulfhydryl reagent. This labeling approach allowed us to determine if the D3 receptor adopted a different conformation and presented different cysteine accessibilities under the three different conditions. The experiments were done using wild type D3 receptors and mutant D3 receptors that do not exhibit tolerance. The results were further confirmed using a D3 receptor agonist that does not induce tolerance in wild type receptors. Together the results strongly support our hypothesis that the D3 receptor adopts a distinct conformational state during tolerance.

Typically receptor signaling is terminated via desensitization mechanisms that involve receptor internalization [21–23]; however, previous studies have shown that D3 receptor undergoes limited agonist-induced internalization [5,8,24]. This raises the question as to how the D3 receptor that is retained on the cell surface terminates its signaling. The results presented here suggest that termination of D3 receptor signaling due to tolerance is likely mediated by a change in receptor conformation that uncouples the receptor from the signaling mechanism. We have previously shown that mutation of a phosphorylation site proximal to the C147 residue attenuates tolerance [5]. This suggests that the conformation adopted during tolerance might be induced by a

change in phosphorylation status of the D3 receptor. We are currently testing this hypothesis.

In summary, in this paper we report the development of a new approach to probe the conformation states adopted by the D3 dopamine receptor under various treatment conditions. Using this approach we showed that the D3 dopamine receptor adopts a distinct conformation state when it undergoes tolerance. We propose that the change in conformation may result in the uncoupling of the D3 receptor from its signal transduction pathways.

Acknowledgments

This work was supported by funding from the F.M. Kirby and UMDNJ Foundation to E.V.K.

References

[1] Missale C, Nash SR, Robinson SW, Jaber M, Caron MG. Dopamine receptors: from structure to function. Physiol Rev 1998;78:189–225.
[2] Neve KA, Seamans JK, Trantham-Davidson H. Dopamine receptor signaling. J Recept Signal Transduct Res 2004;24:165–75.
[3] Cussac D, Newman-Tancredi A, Pasteau V, Millan MJ. Human dopamine D(3) receptors mediate mitogen-activated protein kinase activation via a phosphatidylinositol 3-kinase and an atypical protein kinase C-dependent mechanism. Mol Pharmacol 1999;56:1025–30.
[4] Beom S, Cheong D, Torres G, Caron MG, Kim KM. Comparative studies of molecular mechanisms of dopamine D2 and D3 receptors for the activation of extracellular signal-regulated kinase. J Biol Chem 2004;279:28304–1.
[5] Westrich L, Kuzhikandathil EV. The tolerance property of human D3 dopamine receptor is determined by specific amino acid residues in the second cytoplasmic loop. Biochim Biophys Acta 2007;1773(12):1747–58.
[6] Kuzhikandathil EV, Yu W, Oxford GS. Human dopamine D3 and D2L receptors couple to inward rectifier potassium channels in mammalian cell lines. Mol Cell Neurosci 1998;12:390–2.
[7] Kuzhikandathil EV, Oxford GS. Dominant-negative mutants identify a role for GIRK channels in D3 dopamine receptor-mediated regulation of spontaneous secretory activity. J Gen Physiol 2000;115:697–706.
[8] Kuzhikandathil EV, Westrich L, Bakhos S, Pasuit J. Identification and characterization of novel properties of the human D3 dopamine receptor. Mol Cell Neurosci 2004;26:144–55.
[9] Cherezov V, Rosenbaum DM, Hanson MA, Rasmussen SG, Thian FS, Kobilka TS, et al. High-resolution crystal structure of an engineered human beta2-adrenergic G protein-coupled receptor. Science 2007;318(5854):1258–65.
[10] Eswar N, Marti-Renom MA, Webb B, Madhusudhan MS, Eramian D, Shen M, et al. Comparative protein structure modeling with MODELLER. Current protocols in bioinformatics. John Wiley & Sons Inc.; 2000 [Suppl. 15] p. 5.6.1–30.
[11] Jones G, Willett P, Glen RC, Leach AR, Taylor R. Development and validation of a genetic algorithm for flexible docking. J Mol Biol 1997;267:727–48.
[12] Eldridge MD, Murray CW, Auton TR, Paolinine GV, Mee RP. Empirical scoring functions. I. The development of a fast empirical scoring function to estimate the binding affinity of ligands in receptor complexes. J Comput Aided Mol Des 1997;11(5):425–45.
[13] Kortagere S, Welsh WJ. Development and application of hybrid structure based method for efficient screening of ligands binding to G-protein coupled receptors. J Comput Aided Mol Des 2006;20(12):789–92.
[14] Kalé L, Skeel R, Bhandarkar M, Brunner R, Gursoy A, Krawetz N, et al. NAMD2: greater scalability for parallel molecular dynamics. J Comput Phys 1999;151:283–312.
[15] Brooks BR, Bruccoleri RE, Olafson BD, States DJ, Swaminathan S, Karplus M. CHARMM: a program for macromolecular energy, minimization, and dynamics calculations. J Comput Chem 1983;4:187–217.
[16] Humphrey W, Dalke A, Schulten K. VMD—visual molecular dynamics. J Mol Graph 1996;14:33–8.
[17] Nielsen JE, Andersen KV, Honig B, Hooft RW, Klebe G, Vriend G, et al. Improving macromolecular electrostatics calculations. Protein Eng 1999;12(8):657–62.
[18] Li H, Robertson AD, Jensen JH. Very fast empirical prediction and rationalization of protein pKa values. Proteins 2005;61(4):704–21.
[19] Nebane NM, Hurst DP, Carrasquer CA, Qiao Z, Reggio PH, Song ZH. Residues accessible in the binding-site crevice of transmembrane helix 6 of the CB2 cannabinoid receptor. Biochemistry 2008;47(52):13811–2.
[20] Liapakis G, Simpson MM, Javitch JA. The substituted-cysteine accessibility method (SCAM) to elucidate membrane protein structure. Curr Protoc Neurosci 1999. Supplement 8, Chap. 4, Unit 4.15, pp. 4.15.1–4.15.10..
[21] Gainetdinov RR, Premont RT, Bohn LM, Lefkowitz RJ, Caron MG. Desensitization of G protein-coupled receptors and neuronal functions. Ann Rev Neurosci 2004;27:107–44.
[22] Lefkowitz RJ. G protein-coupled receptors. III. New roles for receptor kinases and beta-arrestins in receptor signaling and desensitization. J Biol Chem 1998;273:18677–80.
[23] Ferguson SS. Evolving concepts in G protein-coupled receptor endocytosis: the role in receptor desensitization and signaling. Pharmacol Rev 2001;53:1–24.
[24] Kim KM, Valenzano KJ, Robinson SR, Yao WD, Barak LS, Caron MG. Differential regulation of the dopamine D2 and D3 receptors by G protein-coupled receptor kinases and beta-arrestins. J Biol Chem 2001;276:37409–14.